Electronic Supplementary Material (ESI) for Journal of Materials Chemistry B.

Structural and biofunctional evaluation of decellularized jellyfish matrices

Jie Zhao[a,#], Wenjun Yu[a,b,#], Qi Zhang[a], Xiaojing Li[a], Yongjie Huang[a], Suwen Zhao[a], Tao Li[c], Shanshan Liu[d,*], Yang Li[a,b,c,*], and Hong Shan[a,e,*]

[a]Guangdong Provincial Engineering Research Center of Molecular Imaging, the Fifth Affiliated Hospital, Sun Yat-sen University, Zhuhai, 519000, China
[b]Department of Radiology, the Fifth Affiliated Hospital, Sun Yat-sen University, Zhuhai, 519000, China
[c]Cardiac Surgery and Structural Heart Disease Unit of Cardiovascular Center, the Fifth Affiliated Hospital, Sun Yat-sen University, Zhuhai 519000, China
[d]Surgical Intensive Care Unit of Department of Critical Care Medicine, the Fifth Affiliated Hospital, Sun Yat-sen University, Zhuhai 519000, China
[e]Department of Interventional Medicine, the Fifth Affiliated Hospital, Sun Yat-sen University, Zhuhai, 519000, China

[#]These authors contributed equally to this work.

***Corresponding authors:**

Shanshan Liu, E-mail: liushan2002@sohu.com

Yang Li, E-mail: liyang266@mail.sysu.edu.cn

Hong Shan, E-mail: shanhong@mail.sysu.edu.cn

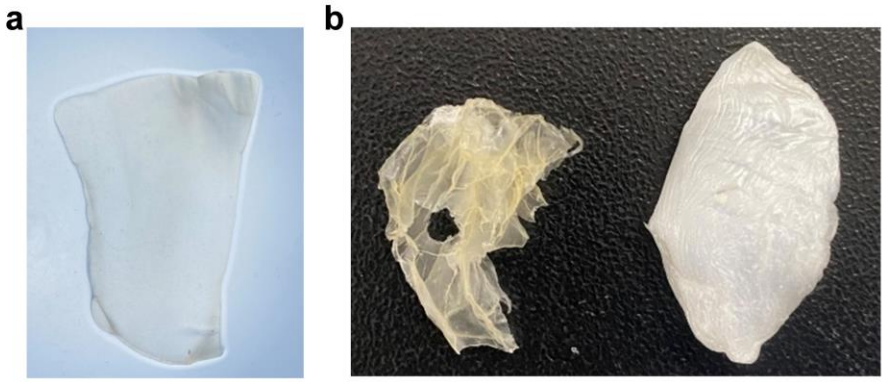

Figure S1. A photograph of an oral arm tissue of jellyfish *R. esculentum* (a) and a photograph of the lyophilized jellyfish matrices with (right) or without (left) EDC crosslinking (b).

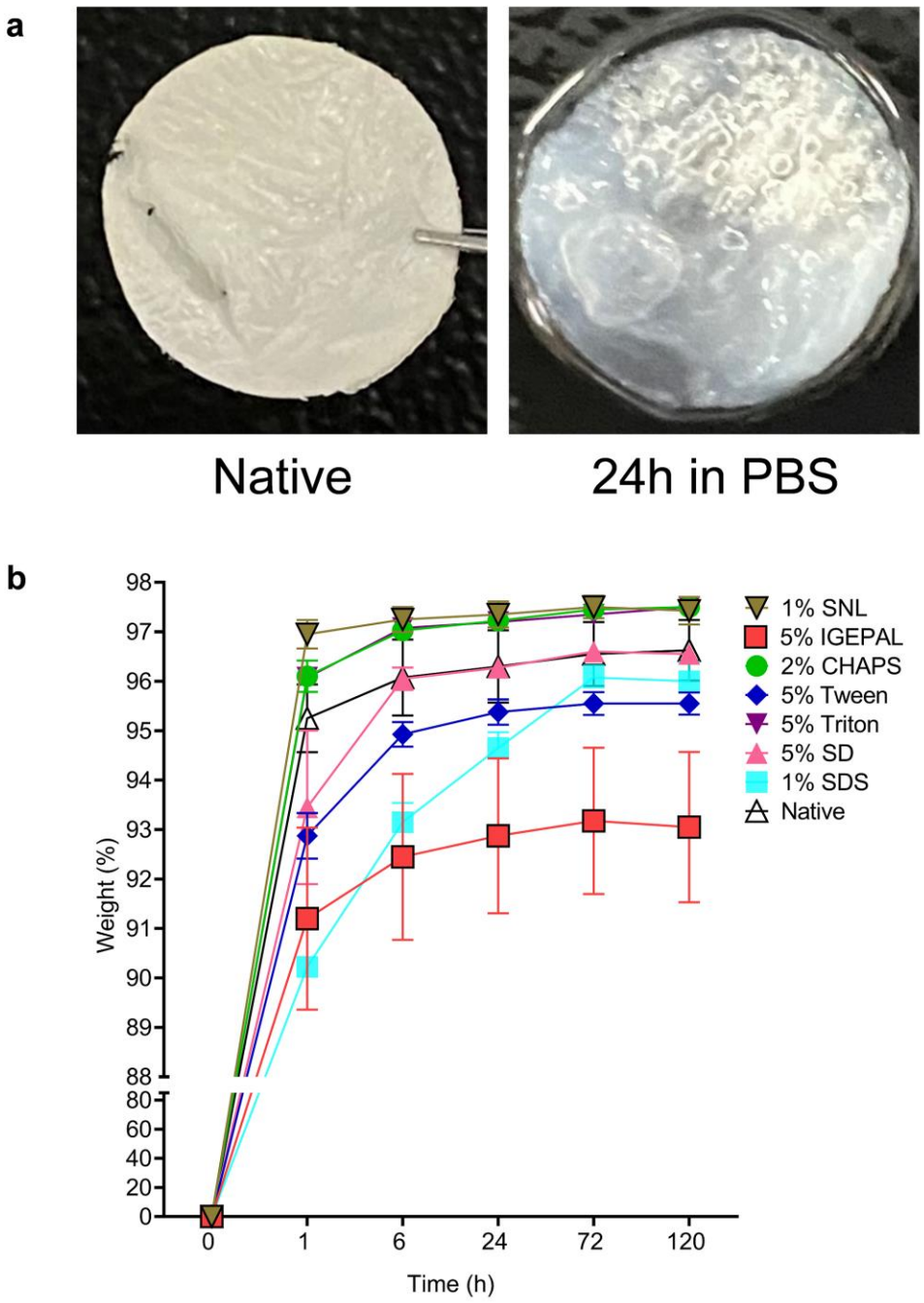

Figure S2. (a) A photograph of a piece of lyophilized jellyfish matrix before (left) and after (right) being immersed in PBS for 24 h. (b) The swelling ratios of the jellyfish scaffolds decellularized with different reagents, indicating the water absorption capacity of the decellularized jellyfish scaffolds. Numbers are presented as mean ± standard error (n = 4).

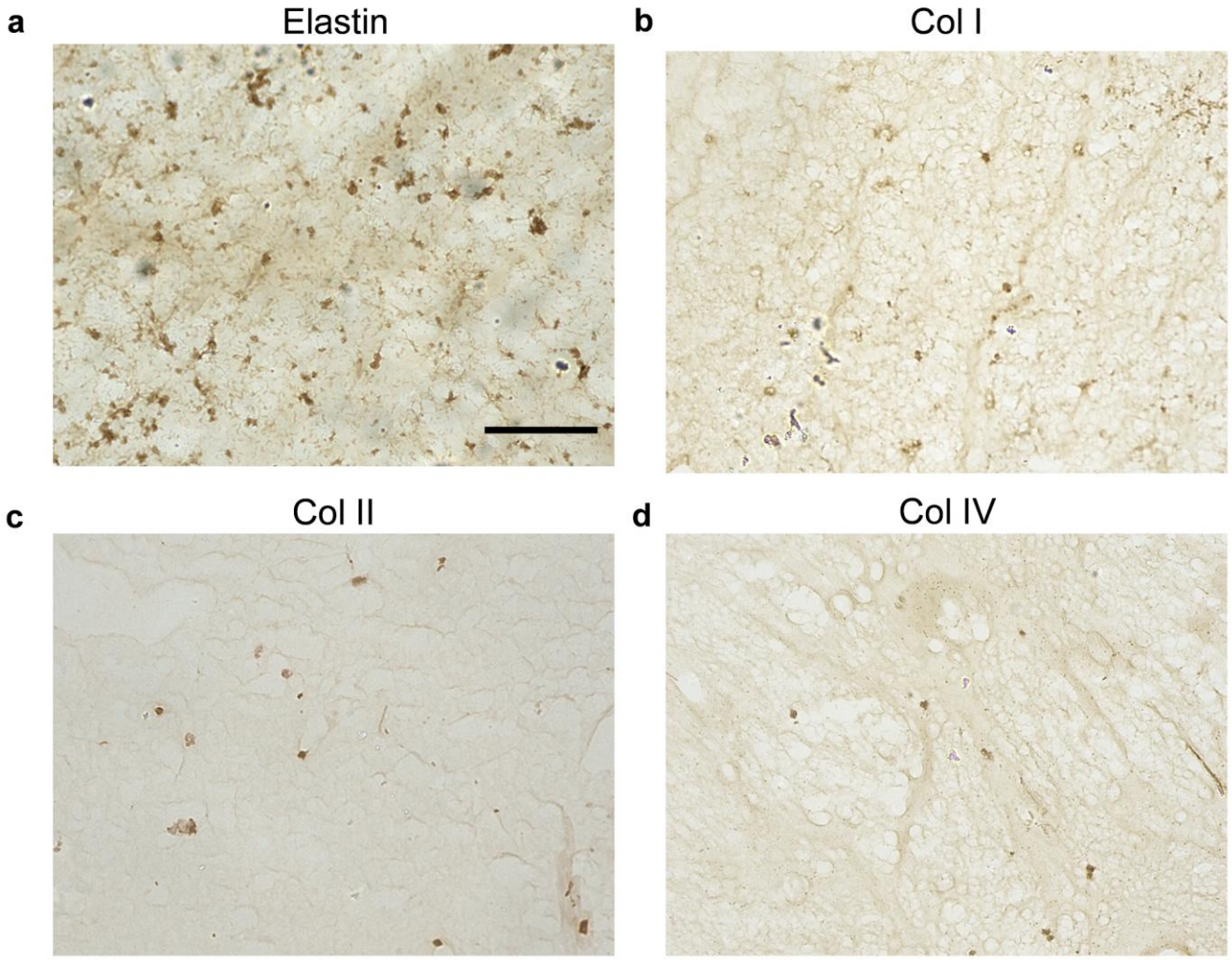

Figure S3. Immunohistochemistry staining of the jellyfish tissue decellularized with 5% SD using antibodies against mammalian elastin (a) as well as type I (b), II (c), and IV (d) collagens. See Methods for the antibody information. Scale bar: 125 μm.

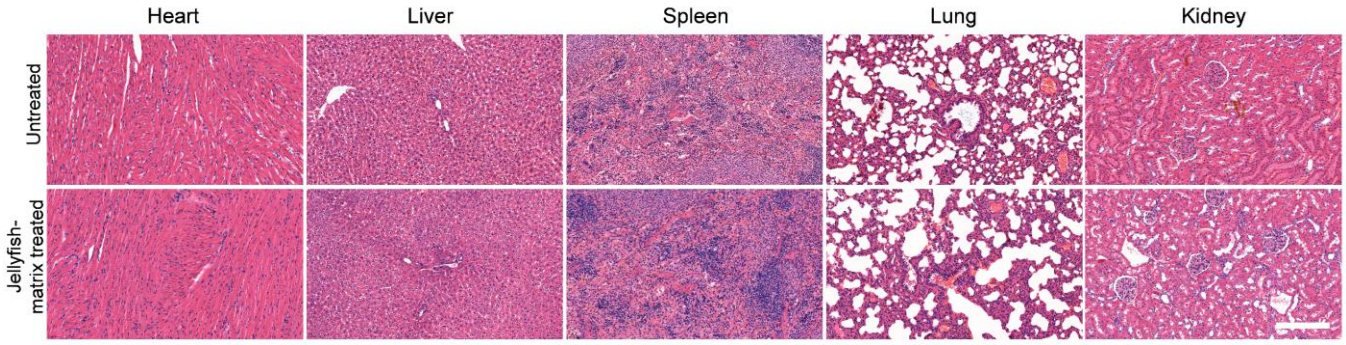

Figure S4. H&E staining of the heart, liver, spleen, lung, and kidney of the rats collected 14 days after wounding and the jellyfish-matrix treatment showing no damage or inflammation in the organs of the jellyfish-matrix treated rats. Scale bar: 100 μm.

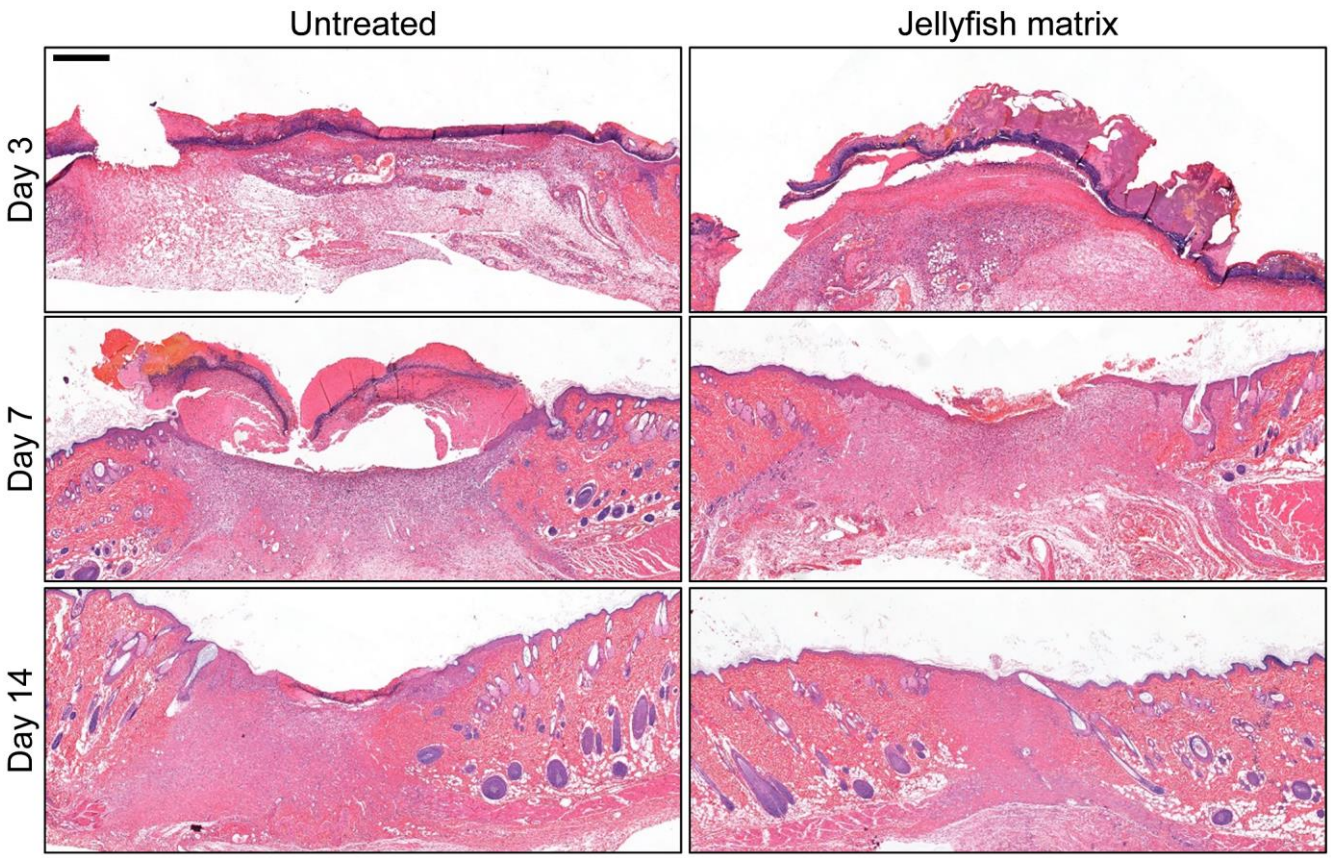

Figure S5. H&E staining of the whole wound beds with the medium healing results from each group on days 3, 7, and 14. Much less exudation was found in the matrix-treated wounds on day 3; more newly formed blood vessels and granulation tissue populated with infiltrating inflammatory cells and fibroblasts were seen in the matrix-treated wound beds on day 7; on day 14, more hair follicles appeared in the jellyfish-matrix treated group. All harvested tissues were fixed in 4% paraformaldehyde for 24 h and dehydrated in gradient alcohol and embedded in paraffin, and then sectioned into 5 μm thickness for the H&E stain. Scale bar: 500 μm.

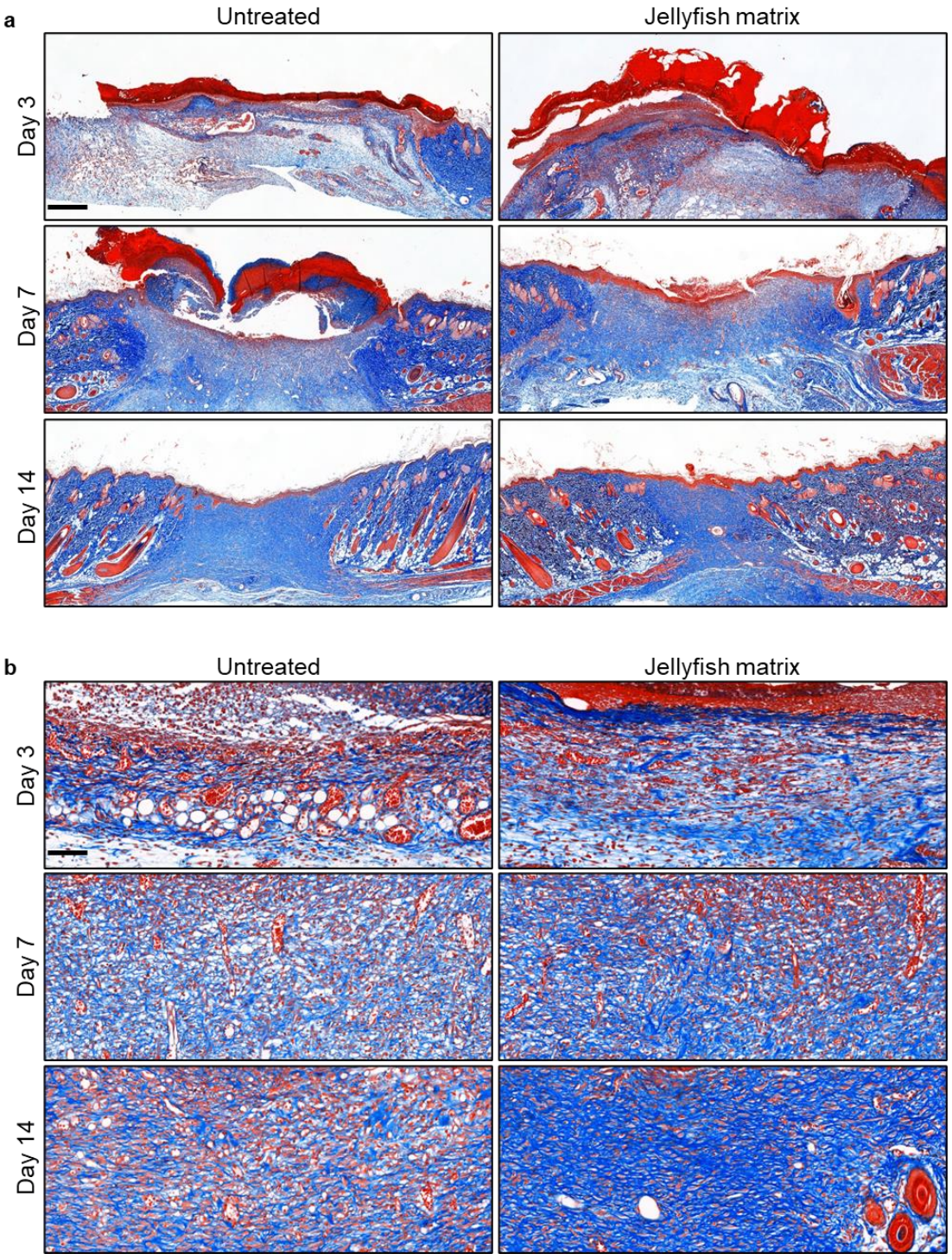

Figure S6. (a) Masson's trichrome staining of the wound beds on days 3, 7, and 14. Scale bar: 500 μm. (b) Representative areas of the wound beds. Scale bar: 100 μm. These Masson's trichrome stain images indicated that the jellyfish-matrix-treated wounds formed denser and more organized collagen fibers on days 7 and 14 compared to the untreated control. All harvested tissues were fixed in 4% paraformaldehyde for 24 h and dehydrated in gradient alcohol and embedded in paraffin, and then sectioned into 5 μm thickness for the staining.

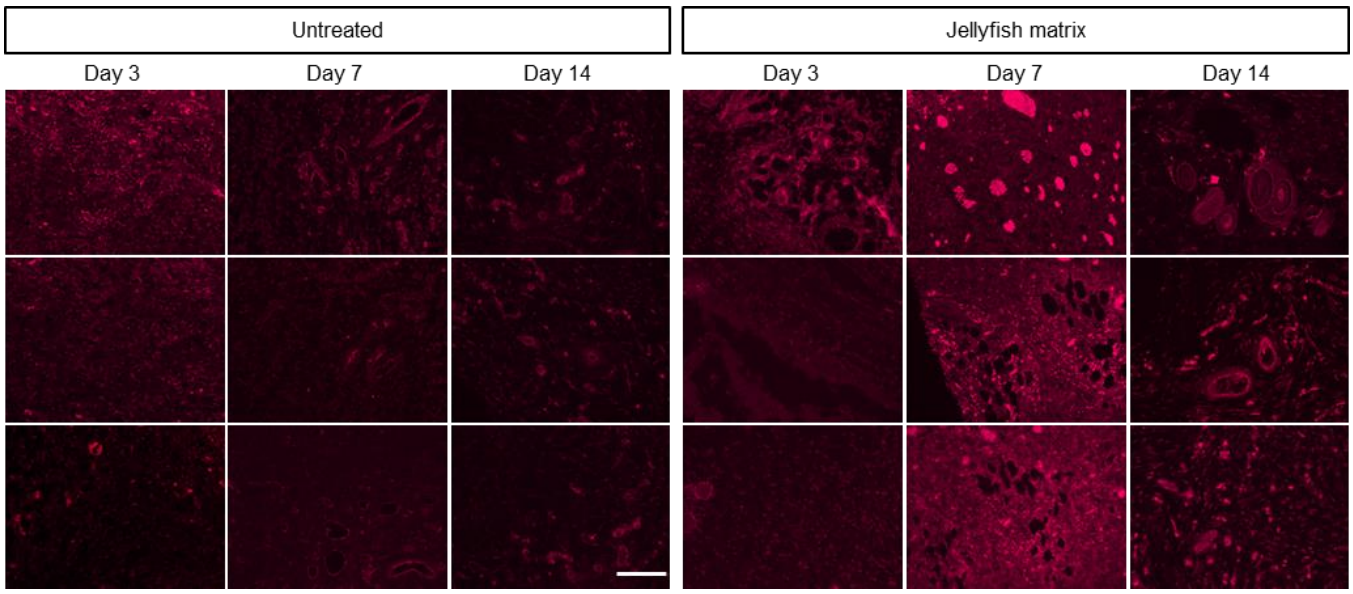

Figure S7. CD31 immunofluorescence staining of the wound beds with medium healing results from each group on days 3, 7, and 14. More CD31-positive blood vessels (pink) were found in the jellyfish-matrix-treated wounds on days 7 and 14, suggesting enhanced angiogenesis compared to the untreated controls. The fixed paraffin-embedded tissue sections on days 3, 7, and 14 were deparaffinized and blocked with 5% goat serum in PBS for 1 h and incubated overnight with the primary antibodies against CD31 (1:500, ab28364, Abcam). The slides were further incubated with a secondary antibody labeled with AlexaFluor647 (ab150079, Abcam). Then the stained slides were rinsed before being mounted with an antifade mounting medium (Vector laboratories, H-1000) and scanned using an EVOS M7000 fluorescence microscope. Scale bar: 125 μm.

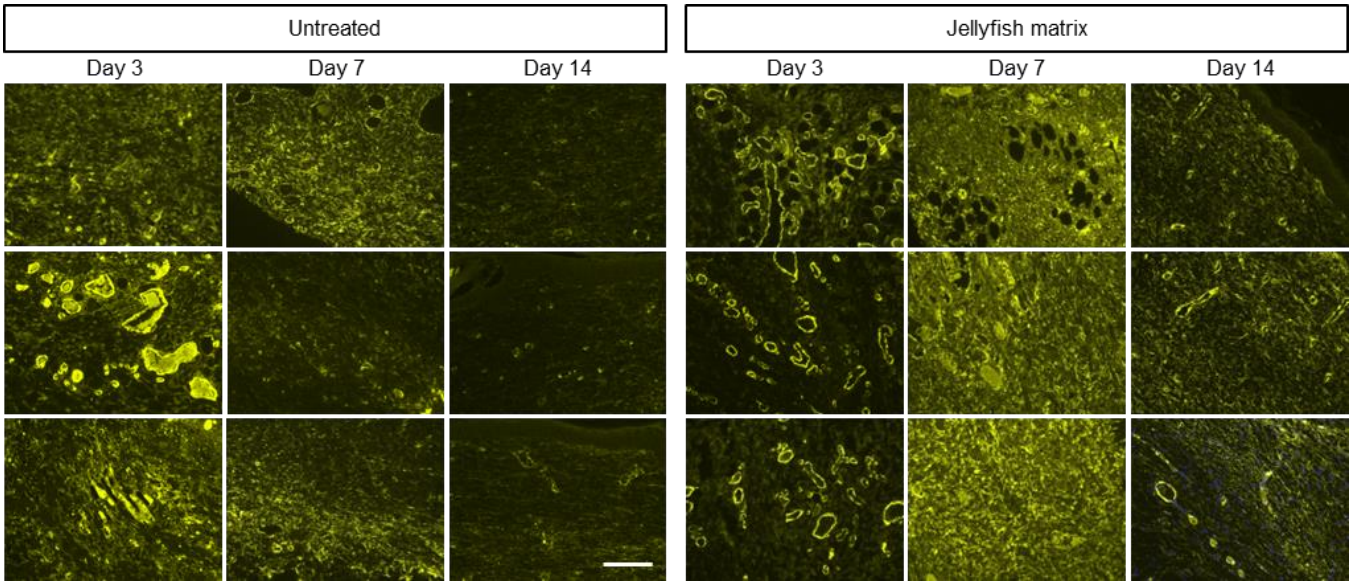

Figure S8. α-SMA immunofluorescence staining of the wound beds with medium healing results from each group on days 3, 7, and 14. Drastically upregulated α-SMA-positive fibroblasts were found in the jellyfish-matrix treated wounds on days 7 and 14, suggesting enhanced ECM production and tissue remodeling in comparison to the untreated controls. The fixed paraffin-embedded tissue sections on days 3, 7, and 14 were deparaffinized and blocked with 5% goat serum and incubated overnight with the primary antibodies against α-SMA (1:500, ab124964, Abcam). The slides were further incubated with a secondary antibody labeled with AlexaFluor647 (ab150079, Abcam) and mounted with an antifade mounting medium (Vector laboratories, H-1000) before being scanned with an EVOS M7000 fluorescence microscope. Scale bar: 125 μm.

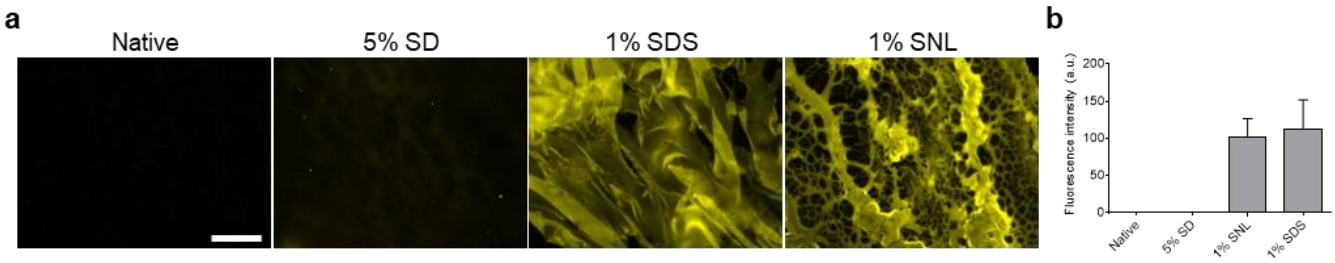

Figure S9. (a) Representative fluorescence images of the native jellyfish tissue or its ECMs decellularized with 5% SD, 1% SDS, or 1% SNL and stained with the biotin-labeled collagen hybridizing peptide (CHP). The CHP binding was further detected with AlexaFluor647-labeled streptavidin. Scale bar: 250 μm. (b) The integrated fluorescence signals quantified from the images from six random locations within each tissue section. This result showcased that the denatured collagen content in the decellularized jellyfish matrices could be exploited to immobilize functional moieties (including but not limited to biotin or streptavidin) non-covalently to the scaffolds, taking advantage of the CHP's triple-helical hybridization with the denatured collagen.